

# Quantum Cross Nonlinearity for Photon-Number-Resolving Nondestructive Detection

Jiang-Shan Tang,<sup>1,2</sup> Mingyuan Chen,<sup>1</sup> Miao Cai,<sup>1</sup> Lei Tang,<sup>1</sup> Yan-Qing Lu,<sup>1,\*</sup> Keyu Xia,<sup>1,2,3,†</sup> and Franco Nori<sup>4,5,‡</sup>

<sup>1</sup>College of Engineering and Applied Sciences, National Laboratory of Solid State Microstructures, and Collaborative Innovation Center of Advanced Microstructures, Nanjing University, Nanjing 210023, China

<sup>2</sup>Hefei National Laboratory, Hefei 230088, China

<sup>3</sup>Shishan Laboratory, Suzhou Campus of Nanjing University, Suzhou 215000, China

<sup>4</sup>Quantum Computing Center, Cluster for Pioneering Research, RIKEN, Wako-shi, Saitama 351-0198, Japan

<sup>5</sup>Physics Department, The University of Michigan, Ann Arbor, Michigan 48109-1040, USA

(Dated: August 16, 2024)

We present an unconventional mechanism for quantum nonlinearity in a system comprising of a V-type quantum emitter (QE) and two Fabry-Pérot cavities. The two transitions of the V-type QE are effectively coupled with two independent cavity modes. The system exhibits a strong quantum nonlinear control in the transmission even at the single-photon level, which we refer to as *quantum cross nonlinearity*. The underlying physics can be understood as *quantum competition* between the two transitions of the QE sharing a common ground state. By leveraging this quantum cross nonlinearity, we further show photon-number-resolving quantum nondestructive detection. Owing to the widespread nature of this V-type configuration, our approach can be readily extended to diverse cavity quantum electrodynamic systems beyond the realm of optics, encompassing, e.g., microwave photons and acoustic wave phonons. This versatility may facilitate numerous unique applications for quantum information processing.

*Introduction.*—Achieving strong nonlinearity between two electromagnetic fields, particularly at the single-photon level, is a longstanding goal in quantum optics, but remains a challenge [1]. Attempts to access a strong nonlinearity in a classical optical medium have been proven exceedingly challenging for light fields with a small number of photons [2].

Relevant advancements in quantum optics have illuminated a viable pathway to attain nonlinearity at the quantum level. The exploitation of anharmonic energy-level splitting, mechanical motion and the excitation-saturation effect in two-level quantum emitters (QEs) to induce quantum nonlinearity has garnered widespread attention, because of the important applications in photon blockade and quantum nonreciprocity [3–14]. Giant Kerr nonlinearity based on electromagnetically induced transparency has also been well understood through quantum interference effects [15–25], but mostly accessible in an ensemble of N-type atoms except for superconducting artificial atoms [21]. Therefore, the demand for novel quantum nonlinear mechanisms remains a longstanding and ongoing endeavor. These efforts hold great promise for both fundamental research and technological applications, including single-photon switches and transistors [26, 27], all-optical deterministic quantum logic gates [28, 29], and strongly correlated states [30–32]. Additionally, these methods provide an opportunity for mutual control of quantum probe fields [33, 34], crucial for quantum nondemolition (QND) measurement [35].

Photon-number-resolving measurements are essential for studying fundamental quantum physics and quantum information technologies. However, most of these measurements rely on the absorption of photons [36–38]. QND measurement of photons promises more exotic applications as it allows for the repeated use of photons, thereby greatly enhancing quantum information processing. For an electromagnetic-field mode, nondestructive detection involves monitoring the

photon number of signal fields without changing them [39–42]. Thanks to the enhanced light-matter interaction within cavities, QND detection of photons has been experimentally demonstrated in various configurations in the microwave domain, including dispersion-shifted two-level QEs [43] and phase-sensitive ladder three-level QEs [35, 42, 44]. The application of optical Kerr nonlinearity to QND measurement is still under debate [45, 46], but single-photon QND can be achieved by combining the quantum nonlocal response with coherently amplified optical Rabi-like coupling in a  $\chi^{(3)}$  nonlinear medium [47–49]. These methods ingeniously harness the nonlinear response encoded in the phase of the probe fields [50]. In stark contrast, the accompanying intensity information of the probe fields is equally important but exclusive in the context of QND measurements. Hence, it is highly desirable to reveal new mechanisms for nondestructive detection of photons by exploring the quantum nonlinearity directly encoded in the probe intensity.

V-type QEs have been explored for achieving QND readout of the qubit state based on the shelving effect [51, 52]. Here, *without* the shelving effect, we show *quantum cross nonlinearity* (QCN) induced in a V-type system, manifested by a mutual nonlinear modulation of the transmission of two probe fields. This quantum nonlinearity originates from the quantum competition between two transition channels sharing the common ground state. QCN is further utilized for photon-number-resolving QND measurements. For a signal field with a small number of photons, the survival rate can exceed 92% by using existing experimental technologies.

*System and model.*—The system configuration is schematically shown in Fig. 1. The two independent Fabry-Pérot (F-P) cavities are formed by two pairs (M1–M2, and M3–M4) of highly reflective mirrors, causing an external loss denoted by  $\kappa_{\text{ex},i}$  ( $i = 1, 2, 3, 4$ ). The two cavity modes, denoted as  $a$  and  $b$ , are characterized by their resonant frequencies,  $\omega_a$  and  $\omega_b$ ,

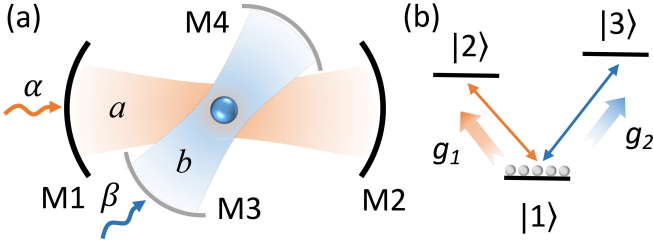


FIG. 1. (a) Schematic diagram for quantum cross nonlinearity and QND measurement of photons. The system consists of two Fabry-Pérot (F-P) cavities, comprising four mirrors M1–M4, and simultaneously coupled to a V-type quantum emitter (QE). The cavity modes are excited by two probe fields  $\alpha$  and  $\beta$ , respectively. (b) Level diagram of the V-type QE, of which two transitions couple to two cavity modes with strengths  $g_1$  and  $g_2$ , respectively.

respectively. The two cavities simultaneously couple with a V-type QE. This QE comprises of a ground state  $|1\rangle$  and two excited states  $|2\rangle$  and  $|3\rangle$ , with corresponding eigenfrequencies  $\omega_1$ ,  $\omega_2$ , and  $\omega_3$ , forming two distinct transitions:  $|1\rangle \leftrightarrow |2\rangle$  and  $|1\rangle \leftrightarrow |3\rangle$ , as depicted in Fig. 1(b). The cavity modes  $a$  and  $b$  couple to distinct transitions of the QE with coupling strengths of  $g_1$  and  $g_2$ , respectively. Such V-type QEs can be realized with atoms [53–57], ions [51], and artificial atoms [10, 52, 58–61], ensuring the broad applicability of our proposal.

We now consider two weak coherent inputs,  $\alpha$  and  $\beta$ , with frequencies  $\omega_{p_1}$  and  $\omega_{p_2}$ . These fields excite cavity modes  $a$  and  $b$  through mirrors M1 and M3, respectively. We denote  $\Delta_a = (\omega_2 - \omega_1) - \omega_a$  and  $\Delta_b = (\omega_3 - \omega_1) - \omega_b$  as the detunings for the cavity modes  $a$  and  $b$  with respect to the transitions  $|1\rangle \leftrightarrow |2\rangle$  and  $|1\rangle \leftrightarrow |3\rangle$ , respectively. The detunings between the cavity modes and the drivings are  $\Delta_1 = \omega_a - \omega_{p_1}$  and  $\Delta_2 = \omega_b - \omega_{p_2}$ , yielding  $\Delta_3 = \Delta_a + \Delta_1$ , and  $\Delta_4 = \Delta_b + \Delta_2$ . In the rotating frame, defined by the unitary transformation  $U = \exp\{i[\omega_{p_1}a^\dagger a + \omega_{p_2}b^\dagger b + \omega_1\sigma_{11} + (\omega_1 + \omega_{p_1})\sigma_{22} + (\omega_1 + \omega_{p_2})\sigma_{33}]\}t$ , the system Hamiltonian takes the form ( $\hbar = 1$ )  $H_S = H_{\text{QCN}} + H_D$ , with the QE-cavity part  $H_{\text{QCN}} = \Delta_1 a^\dagger a + \Delta_2 b^\dagger b + \Delta_3 \sigma_{22} + \Delta_4 \sigma_{33} + g_1 (\sigma_{21} a + a^\dagger \sigma_{12}) + g_2 (\sigma_{31} b + b^\dagger \sigma_{13})$ , for inducing the QCN, and the driving part  $H_D = i\sqrt{\kappa_{\text{ex},1}}(\alpha^* a - \alpha a^\dagger) + i\sqrt{\kappa_{\text{ex},3}}(\beta^* b - \beta b^\dagger)$ , for probing. Here,  $\sigma_{mn} = |m\rangle\langle n|$ ,  $m$  and  $n \in \{1, 2, 3\}$ . The system dynamics can be described by the quantum master equation of the density matrix  $\rho$  as

$$\dot{\rho} = -i[H_S, \rho] + \mathcal{L}\{\Gamma, O\}\rho, \quad (1)$$

where  $\Gamma = \{\kappa_a, \kappa_b, \gamma_{21}, \gamma_{31}\}$  and  $O = \{a, b, \sigma_{12}, \sigma_{13}\}$ ,  $\gamma_{21}$  and  $\gamma_{31}$  describe the decay rates of the two excited states to the ground state, respectively. The Lindblad operator is expressed as  $\mathcal{L}\{\Gamma, O\}\rho = (\Gamma/2)(2O\rho O^\dagger - O^\dagger O\rho - \rho O^\dagger O)$ . The total losses of the cavity modes  $a$  and  $b$  are respectively given by  $\kappa_a = \kappa_{\text{ex},1} + \kappa_{\text{ex},2} + \kappa_{\text{in},a}$  and  $\kappa_b = \kappa_{\text{ex},3} + \kappa_{\text{ex},4} + \kappa_{\text{in},b}$ . The intrinsic losses,  $\kappa_{\text{in},a}$  and  $\kappa_{\text{in},b}$  of cavity fields, are negligible.

Using the input-output relations  $a_t = \sqrt{\kappa_{\text{ex},2}}a$  and  $b_t = \sqrt{\kappa_{\text{ex},4}}b$  [62, 63], we can derive the analytical expressions for

the steady-state transmissions, denoted as  $T_a = \langle a_t^\dagger a_t \rangle / |\alpha|^2$  and  $T_b = \langle b_t^\dagger b_t \rangle / |\beta|^2$  [64], respectively. Furthermore, a fully quantum treatment allows us to numerically solve Eq. (1) by truncating the Fock states of the cavity fields [4].

Next, we examine the time-dependent dynamic evolution of the system when the input signal is a quantum field with the quantum cascaded method [63–67]. In simulations, the coherent input fields are modeled by fields from two virtual “source” cavities  $d_1$  and  $d_2$ , which can numerically generate quantum fields. We use the Hamiltonians  $H_{d_1}$  and  $H_{d_2}$  (see the supplementary material) modeling the source cavities  $d_1$  and  $d_2$  to replace the classical driving  $H_D$ . The master equation describing the quantum cascaded system reads

$$\begin{aligned} \dot{\rho}_{\text{qcs}} = & -i[H_{\text{QCN}}, \rho_{\text{qcs}}] - i[H_{d_1}, \rho_{\text{qcs}}] - i[H_{d_2}, \rho_{\text{qcs}}] \\ & + \mathcal{L}\{\Gamma_{\text{qcs}}, O_{\text{qcs}}\}\rho_{\text{qcs}} + \mathcal{L}_{\text{Net},a}\rho_{\text{qcs}} + \mathcal{L}_{\text{Net},b}\rho_{\text{qcs}}, \end{aligned} \quad (2)$$

where the symbol  $\rho_{\text{qcs}}$  is the joint density matrix of the source cavity modes and the main system for the QCN, the Lindblad terms are  $\mathcal{L}\{\Gamma_{\text{qcs}}, O_{\text{qcs}}\}\rho_{\text{qcs}} = (\Gamma_{\text{qcs}}/2)(2O_{\text{qcs}}\rho_{\text{qcs}}O_{\text{qcs}}^\dagger - O_{\text{qcs}}^\dagger O_{\text{qcs}}\rho_{\text{qcs}} - \rho_{\text{qcs}}O_{\text{qcs}}^\dagger O_{\text{qcs}})$  ( $\Gamma_{\text{qcs}} = \{\kappa_{d_1}, \kappa_{d_2}, \kappa_a, \kappa_b, \gamma_{21}, \gamma_{31}\}$  and  $O_{\text{qcs}} = \{d_1, d_2, a, b, \sigma_{12}, \sigma_{13}\}$ ),  $\mathcal{L}_{\text{Net},a}\rho_{\text{qcs}} = \sqrt{\kappa_{d_1, \text{ex},2}}\kappa_{\text{ex},1}([a^\dagger, d_1\rho_{\text{qcs}}] + [\rho_{\text{qcs}}d_1^\dagger, a])$ , and  $\mathcal{L}_{\text{Net},b}\rho_{\text{qcs}} = \sqrt{\kappa_{d_2, \text{ex},2}}\kappa_{\text{ex},3}([b^\dagger, d_2\rho_{\text{qcs}}] + [\rho_{\text{qcs}}d_2^\dagger, b])$ , where  $\kappa_{d_{i/2}, \text{ex},i}$  ( $i = 1, 2, 3, 4$ ), and  $\kappa_{d_{i/2}}$  represent the external and total attenuations of the source cavities, respectively.

We present a full quantum description of the input and output modes by numerically solving Eq. (2) in the truncated photon-number state basis of the cavity modes. The input-output relations in the cascaded system are [67, 68]

$$\begin{aligned} d_{1,\text{out}} &= \sqrt{\kappa_{d_1, \text{ex},2}}d_1, \quad d_{2,\text{out}} = \sqrt{\kappa_{d_2, \text{ex},2}}d_2, \\ a_t &= \sqrt{\kappa_{\text{ex},2}}a, \quad a_r = \sqrt{\kappa_{d_1, \text{ex},2}}d_1 + \sqrt{\kappa_{\text{ex},1}}a, \\ b_t &= \sqrt{\kappa_{\text{ex},4}}b, \quad b_r = \sqrt{\kappa_{d_2, \text{ex},2}}d_2 + \sqrt{\kappa_{\text{ex},3}}b, \end{aligned} \quad (3)$$

with “ $t$ ” and “ $r$ ” denoting the transmission and reflection coefficients. The operators  $d_{1,\text{out}}$  and  $d_{2,\text{out}}$  describe photons incoming from the source cavities to the QE-cavity subsystem. Thus, for a signal pulse existing from  $t_0$  to  $t_1$ , the transmittance and reflectance of the cavity modes  $a$  and  $b$  can be defined as  $T_s = \int_{t_0}^{t_1} \langle s_r^\dagger s_r \rangle / \int_{t_0}^{t_1} \langle d_{1,\text{out}}^\dagger d_{1,\text{out}} \rangle$  and  $R_s = \int_{t_0}^{t_1} \langle s_r^\dagger s_r \rangle / \int_{t_0}^{t_1} \langle d_{1,\text{out}}^\dagger d_{1,\text{out}} \rangle$  ( $s = a, b$ ), respectively.

**Quantum Cross Nonlinearity.**—Below we consider symmetric F-P cavities so that  $\kappa_{\text{ex},1} = \kappa_{\text{ex},2}$  and  $\kappa_{\text{ex},3} = \kappa_{\text{ex},4}$ , and  $\Delta_a = \Delta_b = 0$  for simplicity. Under the bare-cavity approximation without the QE [64], we obtain the mean photon numbers of the two cavities  $\langle a^\dagger a \rangle \approx 2|\alpha|^2/\kappa_a$  and  $\langle b^\dagger b \rangle \approx 2|\beta|^2/\kappa_b$ . Here,  $|\alpha|^2$  and  $|\beta|^2$  are the input photon fluxes, corresponding to the input power [4, 6, 69]. By solving the steady state of Eq.(1), the transmissions for the cavity modes  $a$  and  $b$  at resonance ( $\Delta_1 = \Delta_2 = 0$ ) are then given by [64]

$$T_a = 1 - 8g_1^2(\kappa_b/\kappa_a)(\gamma_{21}\kappa_a + 2g_1^2)/\mathcal{D}, \quad (4a)$$

$$T_b = 1 - 8g_2^2(\kappa_a/\kappa_b)(\gamma_{31}\kappa_b + 2g_2^2)/\mathcal{D}. \quad (4b)$$

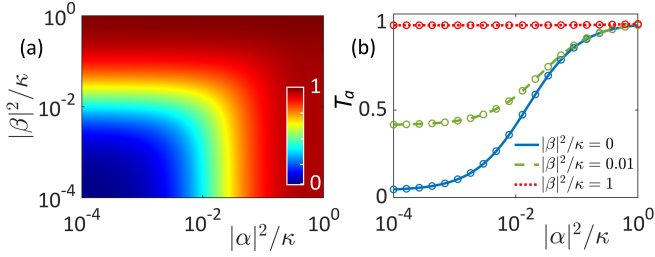


FIG. 2. Quantum cross nonlinearity induced by a V-type QE. (a) Steady-state transmission  $T_a$  versus two input powers,  $|\alpha|^2/\kappa$  and  $|\beta|^2/\kappa$ . (b) Transmission  $T_a$  as a function of  $|\alpha|^2/\kappa$  under different values of  $|\beta|^2/\kappa$ , where curves and open circles are for the analytical and numerical results, respectively. Other parameters:  $\kappa_a = \kappa_b = \kappa$ ,  $\gamma_{21} = \gamma_{31} = 0.01\kappa$ ,  $g_1 = g_2 = 0.1\kappa$ , and  $\Delta_1 = \Delta_2 = \Delta_3 = \Delta_4 = 0$ .

with  $\mathcal{D} = \Gamma_A \Gamma_B \kappa_a \kappa_b + 16(g_1^2 \kappa_b |\alpha|^2 + g_2^2 \kappa_a |\beta|^2)$ ,  $\Gamma_A = \gamma_{21} + 4g_1^2/\kappa_a$  and  $\Gamma_B = \gamma_{31} + 4g_2^2/\kappa_b$ . Note that the term  $g_1^2 \kappa_b |\alpha|^2 + g_2^2 \kappa_a |\beta|^2$  in  $\mathcal{D}$  appearing in the denominator of Eq. (4) indicates the crucial dependence of the transmittances  $T_a$  and  $T_b$  on the excitations of the two cavity modes, despite the *absence* of a direct interaction between them. The conventional classical cross-Kerr nonlinearity has the form of an “Ising”-type interaction,  $\eta^2 \langle a^\dagger a \rangle \langle b^\dagger b \rangle$  [21, 70–72]. Remarkably, the quantum nonlinearity in our system has the form  $\eta_a \langle a^\dagger a \rangle + \eta_b \langle b^\dagger b \rangle$ , originating from quantum competition. Here,  $\eta$ ,  $\eta_a$ , and  $\eta_b$  represent nonlinear coefficients. In this sense, we dub our quantum nonlinearity as “QCN”.

Without loss of generality, we study the quantum nonlinearity of the cavity mode  $a$ , characterized by the nonlinear control of transmittance  $T_a$  with the input fields, as shown in Fig. 2. With identical parameters for the two cavities, the system exhibits a symmetric cross modulation of the transmission  $T_a$  in terms of  $|\alpha|^2/\kappa$  and  $|\beta|^2/\kappa$  [see Fig. 2(a)]. Counter-intuitively, the transmission  $T_a$  can be controlled by the input power  $|\beta|^2/\kappa$ , even in the absence of direct interaction between the cavity modes  $a$  and  $b$  [see Fig. 2(b)]. This cross modulation implies an application in QND measurement. As  $|\beta|^2/\kappa$  increases, the nonlinear curve of  $T_a$  displays an overall rise with a decreasing slope with respect to the input power  $|\alpha|^2/\kappa$ . Intriguingly, the cavity  $a$  can be modified by increasing the driving  $\beta$  to become completely transparent to the incident field  $\alpha$ , even for a weak input power (e.g.,  $|\alpha|^2/\kappa = 10^{-4}$ ), despite initially being almost completely *absorptive*. This means that the amplitude modulation can be close to 100%.

*Quantum Competition.*—The excitation saturation effect causes the quantum nonlinearity mediated by a two-level QE [6, 10, 11]. In stark contrast, the QCN in our V-type configuration results from an essentially different mechanism—quantum competition between two transitions of the V-type QE, because they share a common ground state. Examining the dependence of the excited-state population on the drivings can provide insights into this striking mechanism. In steady

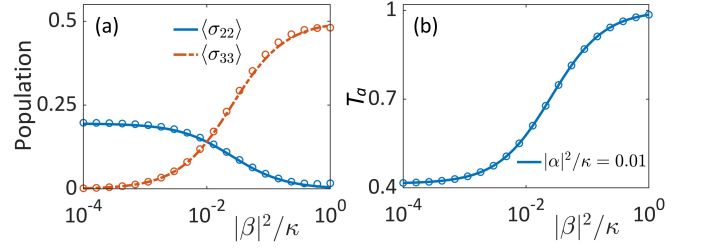


FIG. 3. (a) The population of two excited states of V-type QE, and (b) the transmittance  $T_a$  as a function of the input power  $|\beta|^2/\kappa$ , given a fixed value of  $|\alpha|^2/\kappa = 10^{-2}$ . The analytical results (curves) are in excellent agreement with numerical simulations (dots). Other parameters are the same as those in Fig. 2.

state, the excited states of the QE are populated to [64]

$$\langle \sigma_{22} \rangle = 8g_1^2 \kappa_b |\alpha|^2 / \mathcal{D}, \quad (5a)$$

$$\langle \sigma_{33} \rangle = 8g_2^2 \kappa_a |\beta|^2 / \mathcal{D}. \quad (5b)$$

According to Eq. (5), the excitations,  $\langle \sigma_{22} \rangle$  and  $\langle \sigma_{33} \rangle$ , compete as a function of the two input powers,  $|\alpha|^2/\kappa$  and  $|\beta|^2/\kappa$ . Analytical and numerical results are shown in Fig. 3(a). For input powers  $|\alpha|^2/\kappa = 10^{-2}$  and  $|\beta|^2/\kappa = 0$ , the transition  $|1\rangle \leftrightarrow |2\rangle$  is dominant, leading to  $\langle \sigma_{33} \rangle = 0$ . However, when  $|\beta|^2/\kappa$  increases, the population is gradually “drawn” to the state  $|3\rangle$  by the  $|1\rangle \leftrightarrow |3\rangle$  transition, resulting in a decreasing  $\langle \sigma_{22} \rangle$ . The two excitations reach a balance when  $\alpha = \beta$ . As  $|\beta|^2/\kappa$  increases further, the  $|1\rangle \leftrightarrow |3\rangle$  transition overwhelms the channel  $|1\rangle \leftrightarrow |2\rangle$ , causing the incident field  $\alpha$  to be more likely transmitted compared with the case of the absence of the cavity mode  $b$ , see Fig. 3(b). This quantum competition leads to the nonlinear modulation of  $T_a$  simultaneously by the input powers  $|\alpha|^2/\kappa$  and  $|\beta|^2/\kappa$ , and in turn changes  $T_b$ .

QCN is only applicable in the weak-driving regime. At the small photon-number level, the system displays a cross-nonlinear amplitude modulation. However, with a substantially large influx of photons to the cavities, the QE is saturated, and then is prevented from interacting with additional photons. This saturation results in a unitary transmission, as indicated by Eq. (4). This QCN promises many novel applications, such as QND measurement of photons.

*Photon-Number-Resolving Nondestructive Detection.*—Below, we illustrate how QCN can be leveraged for QND measurement. Here, the two input coherent fields,  $\alpha$  and  $\beta$ , are referred to as the signal field and the probe field, respectively. We consider the signal field as a wave packet containing  $n_s$  ( $n_s = 0, 1, 2, 3, \dots$ ) photons, and the probe field a continuous weak coherent light. To nondestructively resolve the photon number of a signal pulse, we consider a V-type QE situated in two distinct cavities: a single-sided cavity  $a$  [42], featuring one perfectly reflecting mirror and another with a small transmittance for the input and output fields, and a symmetric cavity  $b$  in which both mirrors have identical external coupling rates [64], yielding  $\kappa_a = \kappa_{\text{ex},1} = \kappa$ ,  $\kappa_{\text{ex},2} = 0$ , and  $\kappa_{\text{ex},3} = \kappa_{\text{ex},4} = 0.5\kappa$ . The signal photons are almost entirely



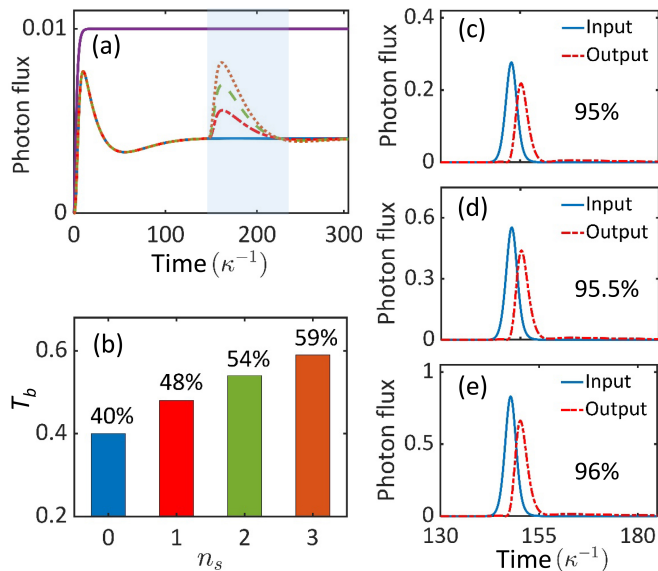


FIG. 4. Photon-number-resolving nondestructive detection based on the QCN. (a) Temporal evolution of the input and output photon fluxes of the probe field. Purple solid curve indicates the probe light incident into the cavity  $b$ . Blue solid, red dash-dotted, green dashed, and orange dotted curves represent the outgoing photon flux of the probe when the signal pulse contains null, one photon, two photons, and three photons, respectively. (b) Probe transmission vs the signal photon numbers. (c)-(e) Temporal evolution of the input and output probe photon fluxes for different signal photon numbers, with (c) representing the one-photon case, (d) the two-photon case, and (e) the three-photon case. Here,  $\kappa_a = \kappa_{\text{ex},1} = \kappa$ ,  $\kappa_{\text{ex},3} = \kappa_{\text{ex},4} = 0.5\kappa$ , and  $|\beta|^2/\kappa = 10^{-2}$ . Other parameters are the same as in Fig. 2.

reflected off the  $a$ -mode cavity, while the transmission of the probe field is modulated by the signal photons via the QCN with a photon-number dependence.

The two cavity modes,  $a$  and  $b$ , do not directly interact with each other and separately couple to different transitions of the QE. An intuitive and transparent physical picture of our proposal can be obtained from the steady-state solutions of the system. It can be seen from Eq. (4b) that the transmittance  $T_b$  of the probe field increases with increasing the excitation of the cavity mode  $a$ , namely, the signal photon number. Once signal photons enters the cavity  $a$ ,  $T_b$  immediately responds. Consequently,  $T_b$  serves as a reliable nondestructive indicator, in real time, for determining the signal photon number.

Using the quantum cascade method [63–65, 67], a full quantum time-domain dynamic evolution simulation is presented in Fig. 4. Due to limitation in computational memory resources, we only simulate the system up to a three-photon signal field [73, 74]. In the absence of signal photons, namely the null-photon case, the probe light reaches a steady-state transmission approximately at  $t = 2\pi \times 120\kappa^{-1}$  [see the blue solid curve in Fig. 4(a)]. To test the modulation of the probe field by a quantum signal, we consider a delayed Gaussian signal pulse, with a delay time  $\tau_d = 2\pi \times 150\kappa^{-1}$  and a pulse duration  $\tau_s = 2\pi \times 6\kappa^{-1}$ . The temporal evolution of the probe transmission is presented in Fig. 4(a). The probe transmissions cor-

responding to different signal photon numbers are indicated by the shadow area. The transmission increases to 48%, 54%, and 59% when the signal pulse includes one, two and three photons, respectively, see Fig. 4(b). This modulation, distinct from the null-photon transmission of 40%, clearly confirms the nondestructive detection of the signal photon numbers.

QND measurements require high survival probability of the signal photons [42]. This survival can be evaluated by the reflectance  $R_a$  of the signal field. Figures 4(c-e) show the input and output signal pulses for  $n_s = 1, 2$  and 3. The corresponding survival probabilities reach 95%, 95.5%, and 96%, respectively, implying a high performance in photon-number-resolving QND measurement. The signal loss attributes to the decay of the state  $|2\rangle$  and the intrinsic loss of the cavity mode  $a$ . Therefore, an effective QND measurement demands the condition  $\gamma_{21}, \kappa_{\text{in},a} \ll \kappa_a$  [64]. Note that our protocol only requires a weak QE-cavity coupling, significantly reducing the difficulty and complexity in experimental implementations.

*Implementation.*—Our QCN requires the two independent transitions of the V-type QE. To meet this requirement, we can separately drive the two transitions with orthogonal polarized cavities [53–56, 59]. An alternative method involves the use of the different transition frequencies, to avoid mutual interference in excitation [52]. For a practical implementation, we further assume that the mirrors M1 – M4 are coated with 99.99%, 99.2%, 99.59%, and 99.59% antireflection dielectric layers, respectively. The cavity length of the two miniature F-P cavities is set to  $400 \mu\text{m}$  [3], yielding  $\kappa_{\text{ex},1} = 2\pi \times 480 \text{ MHz}$ ,  $\kappa_{\text{ex},2} = 2\pi \times 6 \text{ MHz}$ ,  $\kappa_{\text{ex},3} = \kappa_{\text{ex},4} = 2\pi \times 243 \text{ MHz}$ . Considering the impacts of experimental mode matching and other imperfections, we assign a value of  $\kappa_{\text{in},a} = \kappa_{\text{in},b} = 2\pi \times 0.5 \text{ MHz}$  for the intrinsic loss. We consider the  $D_2$  line of a  $^{87}\text{Rb}$  atom for the V-type QE, with levels  $|1\rangle = |5^2S_{1/2}, F = 1, m_F = 0\rangle$ ,  $|2\rangle = |5^2P_{3/2}, F' = 1, m'_F = -1\rangle$ , and  $|3\rangle = |5^2P_{3/2}, F' = 1, m'_F = 1\rangle$ . The corresponding two transitions respectively couple to left- and right-circularly polarized cavity modes, with the same wavelength  $\lambda = 780.2 \text{ nm}$ . The decay rates of the excited states are  $\gamma_{21} = \gamma_{31} = 2\pi \times 3 \text{ MHz}$  [75]. We assume an accessible cavity mode volume of  $10^5 \lambda^3$  [11, 76, 77] and then obtain the coupling strengths up to  $g_1 = g_2 = 2\pi \times 52 \text{ MHz}$ . For these experimental parameters, the survival probability can exceed 92%. In addition, by coupling the V-type superconducting qubits [52, 78] with microwave cavities or surface acoustic wave resonators, QCN can be extended to the domains of microwave photons and phonons.

*Conclusions and outlook.*—We have proposed a striking QCN, originating from the unique mechanism of excitation competition between two quantum transition channels. It enables mutual nonlinear control of two quantum bosonic fields. We have further proved the application of this QCN in the number-resolving QND measurement of traveling bosons, with a high probability of survival.

This novel QCN may offer significant applications in quantum information processing, such as quantum logic gates, single-photon switches, and transistors. In the study of condensed matter electronic systems, the quantum competition

in population of different ground states has been proposed as a means to understand matter phase transitions [79], describe quantum criticality [80], and explore novel matter phases [81]. Exploring quantum competition in a quantum optical system, as a counterpart, can advance the development of strongly correlated many-body quantum systems, quantum phase transitions, and even time crystals [82]. The revealed cross nonlinear interaction among distinct cavity modes may inspire novel quantum nonlinearity topological physics [13, 83, 84] and high-dimensional quantum information processing [85].

This work was supported by the Innovation Program for Quantum Science and Technology (Grant No. 2021ZD0301400), the National Key R&D Program of China (Grants No. 2019YFA0308700), the National Natural Science Foundation of China (Grants No. 12305020 and No. 92365107), the Program for Innovative Talents and Teams in Jiangsu (Grant No. JSSCTD202138), the China Postdoctoral Science Foundation (Grant No. 2023M731613), the Jiangsu Funding Program for Excellent Postdoctoral Talent (Grant No. 2023ZB708), and the Natural Science Foundation of Jiangsu Province, Major Project (Grant No. BK20212004). F. N. is supported in part by Nippon Telegraph and Telephone Corporation (NTT) Research, the Japan Science and Technology Agency (JST) [via the Quantum Leap Flagship Program (Q-LEAP), and the Moonshot R&D Grant No. JP-MJMS2061], the Asian Office of Aerospace Research and Development (AOARD) (via Grant No. FA2386-20-1-4069), and the Office of Naval Research (ONR) (Grant No. N62909-23-1-2074). We thank the High Performance Computing Center of Nanjing University for allowing the numerical calculations on its blade cluster system.

---

\* [yqlu@nju.edu.cn](mailto:yqlu@nju.edu.cn)

† [keyu.xia@nju.edu.cn](mailto:keyu.xia@nju.edu.cn)

‡ [fnori@riken.jp](mailto:fnori@riken.jp)

- [1] T. Peyronel, O. Firstenberg, Q.-Y. Liang, S. Hofferberth, A. V. Gorshkov, T. Pohl, M. D. Lukin, and V. Vuletić, Quantum nonlinear optics with single photons enabled by strongly interacting atoms, *Nature* **488**, 57 (2012).
- [2] D. E. Chang, V. Vuletić, and M. D. Lukin, Quantum nonlinear optics—photon by photon, *Nat. Photonics* **8**, 685 (2014).
- [3] K. M. Birnbaum, A. Boca, R. Miller, A. D. Boozer, T. E. Northup, and H. J. Kimble, Photon blockade in an optical cavity with one trapped atom, *Nature (London)* **436**, 87 (2005).
- [4] B. Dayan, A. S. Parkins, T. Aoki, E. P. Ostby, K. J. Vahala, and H. J. Kimble, A Photon Turnstile Dynamically Regulated by One Atom, *Science* **319**, 1062 (2008).
- [5] P. Rabl, Photon Blockade Effect in Optomechanical Systems, *Phys. Rev. Lett.* **107**, 063601 (2011).
- [6] F. Fratini, E. Mascarenhas, L. Safari, J.-P. Poizat, D. Valente, A. Auffèves, D. Gerace, and M. F. Santos, Fabry-Perot Interferometer with Quantum Mirrors: Nonlinear Light Transport and Rectification, *Phys. Rev. Lett.* **113**, 243601 (2014).
- [7] H. Wang, X. Gu, Y.-x. Liu, A. Miranowicz, and F. Nori, Tunable photon blockade in a hybrid system consisting of an optomechanical device coupled to a two-level system, *Phys. Rev. A* **92**, 033806 (2015).
- [8] C. Hamsen, K. N. Tolazzi, T. Wilk, and G. Rempe, Strong coupling between photons of two light fields mediated by one atom, *Nat. Phys.* **14**, 885 (2018).
- [9] R. Huang, A. Miranowicz, J.-Q. Liao, F. Nori, and H. Jing, Nonreciprocal Photon Blockade, *Phys. Rev. Lett.* **121**, 153601 (2018).
- [10] M. Mirhosseini, E. Kim, X. Zhang, A. Sipahigil, P. B. Dieterle, A. J. Keller, A. Asenjo-Garcia, D. E. Chang, and O. Painter, Cavity quantum electrodynamics with atom-like mirrors, *Nature (London)* **569**, 692 (2019).
- [11] P. Yang, X. Xia, H. He, S. Li, X. Han, P. Zhang, G. Li, P. Zhang, J. Xu, Y. Yang, and T. Zhang, Realization of Nonlinear Optical Nonreciprocity on a Few-Photon Level Based on Atoms Strongly Coupled to an Asymmetric Cavity, *Phys. Rev. Lett.* **123**, 233604 (2019).
- [12] R. Huang, Ş. K. Özdemir, J.-Q. Liao, F. Minganti, L.-M. Kuang, F. Nori, and H. Jing, Exceptional Photon Blockade: Engineering Photon Blockade with Chiral Exceptional Points, *Laser Photon. Rev.* **16**, 2100430 (2022).
- [13] J.-S. Tang, W. Nie, L. Tang, M. Chen, X. Su, Y. Lu, F. Nori, and K. Xia, Nonreciprocal Single-Photon Band Structure, *Phys. Rev. Lett.* **128**, 203602 (2022).
- [14] S. Liu, O. A. D. Sandberg, M. L. Chan, B. Schriniski, Y. Anyfantaki, R. B. Nielsen, R. G. Larsen, A. Skalkin, Y. Wang, L. Miodolo, S. Scholz, A. D. Wieck, A. Ludwig, A. S. Sørensen, A. Tiranov, and P. Lodahl, Violation of Bell inequality by photon scattering on a two-level emitter, *Nat. Phys.* (2024).
- [15] J. Gea-Banacloche, Y.-q. Li, S.-z. Jin, and M. Xiao, Electromagnetically induced transparency in ladder-type inhomogeneously broadened media: Theory and experiment, *Phys. Rev. A* **51**, 576 (1995).
- [16] H. Schmidt and A. Imamoglu, Giant Kerr nonlinearities obtained by electromagnetically induced transparency, *Opt. Lett.* **21**, 1936 (1996).
- [17] A. Imamoglu, H. Schmidt, G. Woods, and M. Deutsch, Strongly Interacting Photons in a Nonlinear Cavity, *Phys. Rev. Lett.* **79**, 1467 (1997).
- [18] S. Rebić, A. S. Parkins, and S. M. Tan, Photon statistics of a single-atom intracavity system involving electromagnetically induced transparency, *Phys. Rev. A* **65**, 063804 (2002).
- [19] H. Kang and Y. Zhu, Observation of Large Kerr Nonlinearity at Low Light Intensities, *Phys. Rev. Lett.* **91**, 093601 (2003).
- [20] H. Wu, J. Gea-Banacloche, and M. Xiao, Observation of Intracavity Electromagnetically Induced Transparency and Polariton Resonances in a Doppler-Broadened Medium, *Phys. Rev. Lett.* **100**, 173602 (2008).
- [21] S. Rebić, J. Twamley, and G. J. Milburn, Giant Kerr Nonlinearities in Circuit Quantum Electrodynamics, *Phys. Rev. Lett.* **103**, 150503 (2009).
- [22] H. Tanji-Suzuki, W. Chen, R. Landig, J. Simon, and V. Vuletić, Vacuum-Induced Transparency, *Science* **333**, 1266 (2011).
- [23] B. Peng, S. K. Özdemir, W. Chen, F. Nori, and L. Yang, What is and what is not electromagnetically induced transparency in whispering-gallery microcavities, *Nat. Commun.* **5**, 5082 (2014).
- [24] A. F. Kockum, A. Miranowicz, V. Macrì, S. Savasta, and F. Nori, Deterministic quantum nonlinear optics with single atoms and virtual photons, *Phys. Rev. A* **95**, 063849 (2017).
- [25] J. Tang, L. Tang, H. Wu, Y. Wu, H. Sun, H. Zhang, T. Li, Y. Lu, M. Xiao, and K. Xia, Towards On-Demand Heralded Single-Photon Sources via Photon Blockade, *Phys. Rev. Appl.* **15**, 064020 (2021).
- [26] J. Hwang, M. Pototschnig, R. Lettow, G. Zumofen, A. Renn,

- S. Götzinger, and V. Sandoghdar, A single-molecule optical transistor, *Nature (London)* **460**, 76 (2009).
- [27] T. Volz, A. Reinhard, M. Winger, A. Badolato, K. J. Hennessy, E. L. Hu, and A. Imamoglu, Ultrafast all-optical switching by single photons, *Nat. Photonics* **6**, 605 (2012).
- [28] M. Hosseini, S. Rebić, B. M. Sparkes, J. Twamley, B. C. Buchler, and P. K. Lam, Memory-enhanced noiseless cross-phase modulation, *Light Sci. Appl.* **1**, e40 (2012).
- [29] A. Reiserer, N. Kalb, G. Rempe, and S. Ritter, A quantum gate between a flying optical photon and a single trapped atom, *Nature (London)* **508**, 237 (2014).
- [30] O. Firstenberg, T. Peyronel, Q.-Y. Liang, A. V. Gorshkov, M. D. Lukin, and V. Vuletić, Attractive photons in a quantum nonlinear medium, *Nature (London)* **502**, 71 (2013).
- [31] S. H. Cantu, A. V. Venkatramani, W. Xu, L. Zhou, B. Jelenković, M. D. Lukin, and V. Vuletić, Repulsive photons in a quantum nonlinear medium, *Nat. Phys.* **16**, 921 (2020).
- [32] Y.-F. Jiao, S.-D. Zhang, Y.-L. Zhang, A. Miranowicz, L.-M. Kuang, and H. Jing, Nonreciprocal Optomechanical Entanglement against Backscattering Losses, *Phys. Rev. Lett.* **125**, 143605 (2020).
- [33] I. Fushman, D. Englund, A. Faraon, N. Stoltz, P. Petroff, and J. Vučković, Controlled Phase Shifts with a Single Quantum Dot, *Science* **320**, 769 (2008).
- [34] L. Tang, J. Tang, M. Chen, F. Nori, M. Xiao, and K. Xia, Quantum Squeezing Induced Optical Nonreciprocity, *Phys. Rev. Lett.* **128**, 083604 (2022).
- [35] G. Nogues, A. Rauschenbeutel, S. Osnaghi, M. Brune, J. M. Raimond, and S. Haroche, Seeing a single photon without destroying it, *Nature (London)* **400**, 239 (1999).
- [36] M. Eaton, A. Hossameldin, R. J. Birrittella, P. M. Alsing, C. C. Gerry, H. Dong, C. Cuevas, and O. Pfister, Resolution of 100 photons and quantum generation of unbiased random numbers, *Nat. Photonics* **17**, 106 (2023).
- [37] R. Cheng, Y. Zhou, S. Wang, M. Shen, T. Taher, and H. X. Tang, A 100-pixel photon-number-resolving detector unveiling photon statistics, *Nat. Photonics* **17**, 112 (2023).
- [38] J. Atalaya, A. Opremcak, A. Nersisyan, K. Lee, and A. N. Korotkov, Measurement of Small Photon Numbers in Circuit QED Resonators, *Phys. Rev. Lett.* **132**, 203601 (2024).
- [39] M. Brune, S. Haroche, V. Lefevre, J. M. Raimond, and N. Zagury, Quantum nondemolition measurement of small photon numbers by rydberg-atom phase-sensitive detection, *Phys. Rev. Lett.* **65**, 976 (1990).
- [40] M. O. Scully and M. S. Zubairy, *Quantum optics* (Cambridge university press, Cambridge, England, 1997).
- [41] G. S. Agarwal, *Quantum optics* (Cambridge University Press, Cambridge, England, 2012).
- [42] A. Reiserer, S. Ritter, and G. Rempe, Nondestructive Detection of an Optical Photon, *Science* **342**, 1349 (2013).
- [43] S. Kono, K. Koshino, Y. Tabuchi, A. Noguchi, and Y. Nakamura, Quantum non-demolition detection of an itinerant microwave photon, *Nat. Phys.* **14**, 546 (2018).
- [44] S. R. Sathyamoorthy, L. Tornberg, A. F. Kockum, B. Q. Baragiola, J. Combes, C. M. Wilson, T. M. Stace, and G. Johansson, Quantum Nondemolition Detection of a Propagating Microwave Photon, *Phys. Rev. Lett.* **112**, 093601 (2014).
- [45] J. H. Shapiro, Single-photon Kerr nonlinearities do not help quantum computation, *Phys. Rev. A* **73**, 062305 (2006).
- [46] J. Gea-Banacloche, Impossibility of large phase shifts via the giant Kerr effect with single-photon wave packets, *Phys. Rev. A* **81**, 043823 (2010).
- [47] K. Xia, M. Johansson, P. L. Knight, and J. Twamley, Cavity-Free Scheme for Nondestructive Detection of a Single Optical Photon, *Phys. Rev. Lett.* **116**, 023601 (2016).
- [48] B. Viswanathan and J. Gea-Banacloche, Analytical results for a conditional phase shift between single-photon pulses in a non-local nonlinear medium, *Phys. Rev. A* **97**, 032314 (2018).
- [49] S. Sagona-Stophel, R. Shahrokhsahi, B. Jordaan, M. Namazi, and E. Figueroa, Conditional  $\pi$ -Phase Shift of Single-Photon-Level Pulses at Room Temperature, *Phys. Rev. Lett.* **125**, 243601 (2020).
- [50] C. Guerlin, J. Bernu, S. Deléglise, C. Sayrin, S. Gleyzes, S. Kuhr, M. Brune, J.-M. Raimond, and S. Haroche, Progressive field-state collapse and quantum non-demolition photon counting, *Nature (London)* **448**, 889 (2007).
- [51] A. H. Myerson, D. J. Szwed, S. C. Webster, D. T. C. Allcock, M. J. Curtis, G. Imreh, J. A. Sherman, D. N. Stacey, A. M. Steane, and D. M. Lucas, High-Fidelity Readout of Trapped-Ion Qubits, *Phys. Rev. Lett.* **100**, 200502 (2008).
- [52] N. Cottet, H. Xiong, L. B. Nguyen, Y. H. Lin, and V. E. Manucharyan, Electron shelving of a superconducting artificial atom, *Nat. Commun.* **12**, 6383 (2021).
- [53] K. Xia, G. Lu, G. Lin, Y. Cheng, Y. Niu, S. Gong, and J. Twamley, Reversible nonmagnetic single-photon isolation using unbalanced quantum coupling, *Phys. Rev. A* **90**, 043802 (2014).
- [54] C. Sayrin, C. Junge, R. Mitsch, B. Albrecht, D. O'Shea, P. Schneeweiss, J. Volz, and A. Rauschenbeutel, Nanophotonic Optical Isolator Controlled by the Internal State of Cold Atoms, *Phys. Rev. X* **5**, 041036 (2015).
- [55] M. Scheucher, A. Hilico, E. Will, J. Volz, and A. Rauschenbeutel, Quantum optical circulator controlled by a single chirally coupled atom, *Science* **354**, 1577 (2016).
- [56] L. Tang, J. Tang, W. Zhang, G. Lu, H. Zhang, Y. Zhang, K. Xia, and M. Xiao, On-chip chiral single-photon interface: Isolation and unidirectional emission, *Phys. Rev. A* **99**, 043833 (2019).
- [57] H. Wu, Y. Ruan, Z. Li, M.-X. Dong, M. Cai, J.-S. Tang, L. Tang, H. Zhang, M. Xiao, and K. Xia, Fundamental Distinction of Electromagnetically Induced Transparency and Autler-Townes Splitting in Breaking the Time-Reversal Symmetry, *Laser Photon. Rev.* **16**, 2100708 (2022).
- [58] J. Q. You, Y.-x. Liu, C. P. Sun, and F. Nori, Persistent single-photon production by tunable on-chip micromaser with a superconducting quantum circuit, *Phys. Rev. B* **75**, 104516 (2007).
- [59] X. Xu, B. Sun, P. R. Berman, D. G. Steel, A. S. Bracker, D. Gammon, and L. J. Sham, Coherent Optical Spectroscopy of a Strongly Driven Quantum Dot, *Science* **317**, 929 (2007).
- [60] H.-C. Sun, Y.-x. Liu, H. Ian, J. Q. You, E. Il'ichev, and F. Nori, Electromagnetically induced transparency and Autler-Townes splitting in superconducting flux quantum circuits, *Phys. Rev. A* **89**, 063822 (2014).
- [61] C.-K. Yong, M. I. B. Utama, C. S. Ong, T. Cao, E. C. Regan, J. Horng, Y. Shen, H. Cai, K. Watanabe, T. Taniguchi, S. Tongay, H. Deng, A. Zettl, S. G. Louie, and F. Wang, Valley-dependent exciton fine structure and Autler-Townes doublets from Berry phases in monolayer MoSe<sub>2</sub>, *Nat. Mater.* **18**, 1065 (2019).
- [62] C. W. Gardiner and M. J. Collett, Input and output in damped quantum systems: Quantum stochastic differential equations and the master equation, *Phys. Rev. A* **31**, 3761 (1985).
- [63] C. W. Gardiner, Driving a quantum system with the output field from another driven quantum system, *Phys. Rev. Lett.* **70**, 2269 (1993).
- [64] See Supplemental Material [url] for the detailed derivations of quantum cross nonlinearity and quantum cascaded simultaion for quantum nondemolition measurement.
- [65] H. J. Carmichael, Quantum trajectory theory for cascaded open

- systems, *Phys. Rev. Lett.* **70**, 2273 (1993).
- [66] H. J. Carmichael, *Statistical Methods in Quantum Optics I: Master Equations and Fokker-Planck Equations* (Springer, Berlin, Heidelberg, 1999).
- [67] X. Su, J.-S. Tang, and K. Xia, Nonlinear dissipation-induced photon blockade, *Phys. Rev. A* **106**, 063707 (2022).
- [68] A. H. Kuilerich and K. Molmer, Input-Output Theory with Quantum Pulses, *Phys. Rev. Lett.* **123**, 123604 (2019).
- [69] J. Dai, A. Roulet, H. N. Le, and V. Scarani, Rectification of light in the quantum regime, *Phys. Rev. A* **92**, 063848 (2015).
- [70] S. Zhang, Y. Hu, G. Lin, Y. Niu, K. Xia, J. Gong, and S. Gong, Thermal-motion-induced non-reciprocal quantum optical system, *Nat. Photonics* **12**, 744 (2018).
- [71] K. Xia, F. Nori, and M. Xiao, Cavity-Free Optical Isolators and Circulators Using a Chiral Cross-Kerr Nonlinearity, *Phys. Rev. Lett.* **121**, 203602 (2018).
- [72] J. Tang, Y. Wu, Z. Wang, H. Sun, L. Tang, H. Zhang, T. Li, Y. Lu, M. Xiao, and K. Xia, Vacuum-induced surface-acoustic-wave phonon blockade, *Phys. Rev. A* **101**, 053802 (2020).
- [73] J. R. Johansson, P. D. Nation, and F. Nori, QuTiP: An open-source Python framework for the dynamics of open quantum systems, *Comput. Phys. Commun.* **183**, 1760 (2012).
- [74] J. R. Johansson, P. D. Nation, and F. Nori, QuTiP 2: A Python framework for the dynamics of open quantum systems, *Comput. Phys. Commun.* **184**, 1234 (2013).
- [75] H. P. Specht, C. Nolleke, A. Reiserer, M. Uphoff, E. Figueroa, S. Ritter, and G. Rempe, A single-atom quantum memory, *Nature (London)* **473**, 190 (2011).
- [76] R. Reimann, W. Alt, T. Kampschulte, T. Macha, L. Ratschbacher, N. Thau, S. Yoon, and D. Meschede, Cavity-Modified Collective Rayleigh Scattering of Two Atoms, *Phys. Rev. Lett.* **114**, 023601 (2015).
- [77] Y. Liu, Z. Wang, P. Yang, Q. Wang, Q. Fan, S. Guan, G. Li, P. Zhang, and T. Zhang, Realization of Strong Coupling between Deterministic Single-Atom Arrays and a High-Finesse Miniature Optical Cavity, *Phys. Rev. Lett.* **130**, 173601 (2023).
- [78] Y. Han, X.-Q. Luo, T.-F. Li, W. Zhang, S.-P. Wang, J. Tsai, F. Nori, and J. You, Time-Domain Grating with a Periodically Driven Qutrit, *Phys. Rev. Appl.* **11**, 014053 (2019).
- [79] H. J. Kang, P. Dai, J. W. Lynn, M. Matsuura, J. R. Thompson, S.-C. Zhang, D. N. Argyriou, Y. Onose, and Y. Tokura, Antiferromagnetic order as the competing ground state in electron-doped  $\text{Nd}_{1.85}\text{Ce}_{0.15}\text{CuO}_4$ , *Nature (London)* **423**, 522 (2003).
- [80] S. Sachdev, Quantum Criticality: Competing Ground States in Low Dimensions, *Science* **288**, 475 (2000).
- [81] I. Hagymasi, M. S. Mohd Isa, Z. Tajkov, K. Marity, L. Oroszlany, J. Koltai, A. Alassaf, P. Kun, K. Kandrai, A. Palinkas, P. Vancso, L. Tapaszto, and P. Nemes-Incze, Observation of competing, correlated ground states in the flat band of rhombohedral graphite, *Sci. Adv.* **8**, eabo6879 (2022).
- [82] X. Wu, Z. Wang, F. Yang, R. Gao, C. Liang, M. K. Tey, X. Li, T. Pohl, and L. You, Dissipative time crystal in a strongly interacting Rydberg gas, *Nat. Phys.* **10**, 1038/s41567-024-02542-9 (2024).
- [83] M. S. Kirsch, Y. Zhang, M. Kremer, L. J. Maczewsky, S. K. Ivanov, Y. V. Kartashov, L. Torner, D. Bauer, A. Szameit, and M. Heinrich, Nonlinear second-order photonic topological insulators, *Nat. Phys.* **17**, 995 (2021).
- [84] K. Sone, M. Ezawa, Y. Ashida, N. Yoshioka, and T. Sagawa, Nonlinearity-induced topological phase transition characterized by the nonlinear Chern number, *Nat. Phys.* **20**, 1164 (2024).
- [85] M. Chen, J.-S. Tang, M. Cai, Y. Lu, F. Nori, and K. Xia, High-dimensional two-photon quantum controlled phase-flip gate, *Phys. Rev. Res.* **6**, 033004 (2024).